A Monte Carlo investigation of the thermodynamics of cation ordering in 2-3 spinels

Erika J. Palin* and Richard J. Harrison

Department of Earth Sciences, University of Cambridge, Downing Street, Cambridge CB2 3EQ, U.K.

Abstract

The Monte Carlo (MC) simulation technique is a powerful tool for the investigation of thermodynamic and kinetic phenomena in minerals, and is especially well suited to the study of cation ordering. We have performed MC simulations of eight end-member 2-3 spinels (X^{2+} = Mg, Fe, Zn, Ni; X^{3+} = Al, Fe) using pair interaction parameters, J_i, and chemical potentials, μ, derived from atomistic simulations. The J_i values for all but one of these spinels are remarkably similar, despite their different character (normal vs. inverse). The sign of μ, and hence the tendency to form a normal or inverse spinel, was correctly predicted in all cases. Agreement between the simulated and observed cation distributions as a function of temperature is good for the normal spinels and poor for the inverse spinels. Agreement could be greatly improved for the inverse spinels through relatively modest adjustments to the simulation parameters (usually increasing the strength of the tetrahedral-octahedral, T-O, interactions, and decreasing the magnitude of μ).

We have developed an atomistic random-mixing model for cation ordering in spinels and compared it with the macroscopic O'Neill-Navrotsky model. In so doing, we have determined the relative contributions of μ, tetrahedral-tetrahedral (T-T), octahedral-octahedral (O-O), and T-O interactions to the O'Neill-Navrotsky coefficients α and β. We found that the value of β depends on the relative enthalpy contributions of (T-T + O-O) vs. T-O interactions, a useful insight considering the large spread of values found experimentally to be taken by β.

We used the thermodynamic integration technique to quantify the entropy, and hence the amount of short-range order, present in the spinels studied. We found that there is virtually no short-range order in the normal spinels. There is significant short-range order in the inverse spinels, though in the experimentally accessible temperature range, the contribution of this short-range order to the entropy is comparatively small. At very low temperatures, we find that the octahedral cations in the inverse spinels become ordered, reducing the symmetry to $P4_122$, in agreement with other simulated findings for 2-3 spinels and experimental findings for 4-2 spinels.

Keywords: Spinel, thermodynamics, Monte Carlo simulation, O'Neill-Navrotsky model, short-range order

Introduction

The spinel structure, with general formula AB_2O_4, is adopted by a variety of materials, including minerals, catalysts, superconductors, magnetic materials, and semiconductors. Ringwoodite, a spinel-structured polymorph of $(Fe,Mg)_2SiO_4$, is an important phase in the lower part of the Earth's transition zone, and spinel-structured minerals can be found in various different classes of igneous and metamorphic rocks, and in several varieties of meteorite.

The spinel structure consists of pseudo-close-packed planes of oxygen anions, in which there are tetrahedral and octahedral interstices where cations can be placed. The A and B cations may be distributed across these tetrahedral and octahedral sites in different ways. A spinel with the configuration $^{IV}A^{VI}B_2O_4$ is termed "normal," while one with the configuration $^{IV}B^{VI}(AB)O_4$ is termed "inverse." The continuum of possible states between these two extremes is quantified by the inversion parameter, x, which

defines the fraction of B cations on tetrahedral sites. Hence, x is zero for a normal spinel, 2/3 for a spinel with completely random configuration, and 1 for a fully inverse spinel. Alternatively, an order parameter Q can be defined, which has value 1 for the normal case, 0 for the random case, and –0.5 for the inverse case. The relationship between x and Q is thus $Q = 1 - 3x/2$.

Considerable research has been conducted into the thermodynamics of cation ordering in minerals with the spinel structure. In particular, the thermodynamic model of O'Neill and Navrotsky (1983) has been shown to be very good at describing ordering in end-member spinels. The O'Neill-Navrotsky model states that the enthalpy of disordering can be represented as a quadratic function of the inversion parameter:

$$\Delta H_D = \alpha x + \beta x^2 \tag{1}$$

where α and β are coefficients that can be determined for a particular spinel from experimental data for the cation distribution as a function of temperature.

The expression for the configurational entropy, assuming

* E-mail: ejp24@cam.ac.uk

completely random mixing of cations across all sites, is

$$S_{conf} = \sum_i nx_i \ln x_i$$

$$= -R\left[x\ln x + (1-x)\ln(1-x) + x\ln\left(\frac{x}{2}\right) + (2-x)\ln\left(1-\frac{x}{2}\right)\right] \quad (2)$$

where n is the number of sites per formula unit. Hence the resulting expression for the free energy relative to the perfectly ordered spinel ($x = 0$) is

$$\Delta G = \Delta H - T\Delta S$$

$$= \alpha x + \beta x^2 + RT\left[x\ln x + (1-x)\ln(1-x) + x\ln\left(\frac{x}{2}\right) + (2-x)\ln\left(1-\frac{x}{2}\right)\right] \quad (3)$$

It was initially suggested that the majority of spinels could be described using a "universal" value of $\beta = -20$ kJ/mol (O'Neill and Navrotsky 1984). Experimental studies have since shown that β can adopt a wide range of both positive and negative values [e.g., +19.7 kJ/mol for $FeAl_2O_4$ (Harrison et al. 1998); +4.7 kJ/mol for $MgAl_2O_4$ (Redfern et al. 1999); −18.4 kJ/mol for $NiAl_2O_4$ (O'Neill et al. 1991); −21.7 kJ/mol for $MgFe_2O_4$ (O'Neill et al. 1992); −34.1 kJ/mol for $ZnFe_2O_4$ (O'Neill 1992)].

In this work, we examine cation ordering in spinels via a Monte Carlo simulation approach. Several types of Monte Carlo simulations have been used to study a variety of mineralogically relevant processes. The "reverse Monte Carlo" technique has been used in conjunction with experimental investigation to examine dynamic disorder and phase transitions in SiO_2 polymorphs (Tucker et al. 2001a, 2001b), and the structures of the octahedral sheet in illite-smectites (Cuadros et al. 1999). "Kinetic Monte Carlo" simulations allow the investigation of crystal growth (e.g., Piana and Gale 2006) and dissolution processes (e.g., Arvidson and Luttge 2004). The "forward Monte Carlo" technique lends itself well to the study of cation ordering; rapid, but thermodynamically accurate, sampling of phase space is possible, and the system evolves relatively quickly toward the equilibrium state. Mineral systems in which the MC technique has already been successfully applied to cation ordering include micas (Palin et al. 2001, 2003b), illite-smectites (Sainz-Díaz et al. 2003a, 2003b, 2004; Palin et al. 2004), amphiboles (Palin et al. 2003a, 2005), ilmenite-hematite (Harrison 2006), and garnets (Bosenick et al. 2000; Vinograd and Sluiter 2006; Vinograd et al. 2006a, 2006b). Previous MC investigations have also been undertaken on spinels (Warren et al. 2000a, 2000b; Lavrentiev et al. 2003), and we discuss these below.

Our aim in this work is to use Monte Carlo simulations to investigate why the O'Neill-Navrotsky model works so well for spinels, and to gain insights into the controls on the variability of α and β. One particular advantage of Monte Carlo simulations in this study is that short-range order is treated correctly, whereas it is not included in the O'Neill-Navrotsky model.

This study is the first step toward an atomistic model of coupled cation and magnetic ordering in spinel solid solutions. A similar approach has recently proved highly successful in the investigation of magnetism and microstructure in the ilmenite-hematite solid solution (Harrison 2006), and we envisage that this study of spinels will be similarly useful in terms of the subsequent investigation we plan to undertake into the effect of cation distributions on magnetic ordering. Recently, Lavrentiev et al. (2003) investigated 2-3 end-member spinels via Monte Carlo simulation, using a technique that considers the effect of vibrational contributions to the lattice energy on the ordering behavior. Our approach, referred to as the J formalism, (Bosenick et al. 2001) describes the thermodynamics of ordering using a set of pair interaction parameters and site preference energies derived from static lattice energy calculations. This approach neglects vibrational contributions to the lattice energy, but has been used successfully in the past to study many other mineral systems, e.g., the clay minerals and amphiboles cited above. In this study we assess whether the same approach is suitable for modeling spinels. By comparing our results with those of Lavrentiev et al. (2003) we demonstrate that vibrational contributions have a relatively minor effect on the calculated cation distributions, an observation that greatly simplifies the computations. We demonstrate a striking similarity between the pair interaction parameters derived for both normal and inverse spinels, and develop a general approach to atomistic modeling of spinels that both closely reproduces experimental data and correctly describes the configurational entropy.

METHOD

J formalism for cation ordering in spinels

The formalism underlying our simulations, which we call the J formalism, has been discussed in detail by Bosenick et al. (2001), so here we simply give a summary. It is possible to express the enthalpy of a system of interacting cations as

$$E = E_0 + \sum_{\langle ij \rangle} N_{ij}^n J_{ij}^n + \sum_j N_j \mu_j \quad (4)$$

where E_0 is a constant term, J_{ij}^n represents the enthalpy of an interaction between two cation species i and j across distance n, N_{ij}^n is the number of interactions of type n, and μ_j is a constant site preference energy (or "chemical potential") describing the energy associated with placing cation j on a given type of site.

Equation 4 can be solved via multi-linear regression. Many different cation configurations are created, and the geometry of each is optimized with the program GULP (Gale 1997) to produce a data set of configurations, each with a different E value. N_{ij} and N_j can be computed (e.g., via a spreadsheet method) for each configuration, and Equation 4 can thus be solved for J_{ij} and μ_j (and E_0, though this constant is not used in any subsequent investigation). These values of J_{ij} and μ_j are then used as input for Monte Carlo simulations.

The first part of the analysis is to identify the distances in the crystal structure for which the interaction parameters J_{ij} are to be defined. To this end, the crystal structure of spinel was examined, and twelve interaction parameters were defined. These are for the four shortest inter-cation distances for each of T-T, O-O, and T-O interactions (T = tetrahedral, O = octahedral), and are listed in Table 1.

TABLE 1. Distances corresponding to J parameters for spinel structure

Parameter	Distance (Å)	Vector type	Number of neighbors
$J_{1,TT}$	3.50	1/4 1/4 1/4	4
$J_{2,TT}$	5.71	1/2 1/2 0	12
$J_{3,TT}$	6.70	3/4 1/4 1/4	12
$J_{4,TT}$	8.08	1 0 0	6
$J_{1,OO}$	2.86	1/4 1/4 0	6
$J_{2,OO}$	4.95	1/4 1/4 1/2	12
$J_{3,OO}$	5.71	1/2 1/2 0	12
$J_{4,OO}$	6.39	3/4 1/4 0	12
$J_{1,TO}$	3.35	3/8 1/8 1/8	12*
$J_{2,TO}$	5.25	5/8 1/8 1/8, 3/8 3/8 3/8	16*
$J_{3,TO}$	6.62	5/8 3/8 3/8	12*
$J_{4,TO}$	7.76	7/8 3/8 1/8, 5/8 5/8 3/8	36*

Note: Distances quoted are based on $MgAl_2O_4$ and will therefore vary for other spinels.

* Counted from T sites. If counted from O sites, halve this number.

Interatomic potential model for spinels

The interatomic potentials used in this work were identical to those derived by Lavrentiev et al. (2003). We used these parameters to study the following compositions: $MgAl_2O_4$ (spinel, normal), $MgFe_2O_4$ (magnesioferrite, inverse), $NiAl_2O_4$ (inverse), $NiFe_2O_4$ (trevorite, inverse), $FeAl_2O_4$ (hercynite, normal), Fe_3O_4 (magnetite, inverse), $ZnAl_2O_4$ (gahnite, normal), and $ZnFe_2O_4$ (normal).

To compute the J parameters, the approach discussed by Bosenick et al. (2001) was used. This involved taking lattice parameters and atomic coordinates from experimental sources, and constructing a unit cell of the fully cation disordered structure using the virtual crystal approximation (VCA). In spinels, this means that each site (both tetrahedral and octahedral) has an occupancy of 1/3 A and 2/3 B. We constructed a $2 \times 2 \times 2$ supercell containing 128 octahedral sites and 64 tetrahedral sites for this purpose. This unit cell was optimized with the program GULP (Gale 1997) at constant pressure, to allow the cell parameters to relax. The experimental parameters used for each spinel, and the output parameters from the GULP optimization, are given in Table 2. The output coordinates and lattice parameters were then used to generate many configurations of the unit cell for each spinel, with randomly located A and B atoms in the structure giving varying degrees of inversion. Twenty configurations at each of $x = 1/16$, 1/8, 3/16, 1/4, 5/16, 3/8, 7/16, 1/2, 9/16, 5/8, 11/16, 3/4, 13/16, 7/8, 15/16, and 1 were generated. This, together with the fully normal structure, gave a data set of 321 configurations for each composition. These configurations were optimized using GULP, and multi-linear regression analysis was used to compute the twelve J values and chemical potential μ.

It is not clear whether, in general, it is better to allow the cell parameters to change during optimization of the random configurations (constant pressure), or to hold them fixed (constant volume) (Bosenick et al. 2001). This is especially relevant here, since we are modeling systems with different degrees of inversion, which may have different cell parameters. We investigated the effect on the J values of calculating them from configurations optimized at constant volume and at constant pressure, and found that there was negligible difference.

Additionally, when placing the cations randomly on the lattice sites to generate the 321 input configurations, we used the same set of random numbers for each different spinel. We tested the effect of using a different set of random numbers for the case of $MgFe_2O_4$, and found that the effect on the J values was, again, negligible.

Once values are calculated for the various parameters, the enthalpy for each configuration can be calculated according to Equation 4, and compared with the actual value from GULP. The quality of the fit between observed and calculated energies can be measured by the R^2 correlation coefficient:

$$R^2 = 1 - \frac{\left\langle (\Delta E)^2 \right\rangle}{\left\langle E^2 \right\rangle - \left\langle E \right\rangle^2} \tag{5}$$

for which a value of 1 indicates a perfect correlation (see Table 3).

Random-mixing model for ordering in spinels

The general spinel formula can be written as $^{IV}(A_{1-x}B_x)^{VI}(A_{1-x/2}B_{x/2})_2O_4$, where x is the degree of inversion. From this general formula, a model for the system enthalpy can be derived, assuming completely random mixing of cations on each of the two sublattices. This model can then be compared with the O'Neill-Navrotsky model, and serves as a predictive tool for the simulation results (remembering that the model neglects the possibility of short-range order).

In a spinel with degree of inversion x, we can formulate an expression for the enthalpy depending on the probability of finding an interaction between two unlike atoms across a particular distance. First, the probability of finding an interaction of a particular type can be expressed as the probability of finding a particular atom on a particular site multiplied by the probability of finding a neighbor of the opposite type. The former quantity is given by the site occupancy in the general

chemical formula (e.g., probability of finding a B atom on a tetrahedral site $= x$), and the latter is dependent on the number of neighbors of a particular site across a particular distance (e.g., probability of finding an A neighbor in a tetrahedral site across a J_1 distance $= (1-x)z_{1,TT}$, where $z_{1,TT}$ = the number of nearest-neighbor tetrahedral sites). The enthalpy of a particular interaction is just the probability of that interaction multiplied by the J value for that interaction, e.g., for an A-B nearest-neighbor T-T interaction, the enthalpy is $4x(1-x)J_{1,TT}$, where $z_{1,TT} = 4$ (Table 1).

Extending this to include (1) further than nearest-neighbor interactions; (2) interactions of all types (T-T, O-O, T-O); and (3) all the tetrahedral and octahedral sites present, we obtain

$$E_J = N_T x(1-x)\left(4J_{1,TT} + 12J_{2,TT} + 12J_{3,TT} + 6J_{4,TT}\right)$$
$$+ N_O \cdot \frac{x}{2} \cdot \left(1 - \frac{x}{2}\right)\left(6J_{1,OO} + 12J_{2,OO} + 12J_{3,OO} + 12J_{4,OO}\right) \tag{6}$$
$$+ N_T\left[\frac{x^2}{2} + (1-x)\left(1-\frac{x}{2}\right)\right]\left(12J_{1,TO} + 16J_{2,TO} + 12J_{3,TO} + 36J_{4,TO}\right)$$

where N_T and N_O are the numbers of tetrahedral and octahedral sites.

We also need to quantify the enthalpy contribution from moving atoms between tetrahedral and octahedral sites, i.e., the chemical potential. We define our chemical potential to be for B atoms on tetrahedral sites (e.g., Al on tetrahedral sites for $MgAl_2O_4$, Fe on tetrahedral sites for $MgFe_2O_4$, etc.). A negative chemical potential therefore favors B atoms on tetrahedral sites, i.e., the inverse case, and a positive chemical potential disfavors B atoms on tetrahedral sites, i.e., the normal case. The enthalpy contribution from the chemical potential is

$$E_μ = N_T μx \tag{7}$$

such that the maximum contribution (be it positive or negative) from this term occurs for the fully inverse spinel, and there is no contribution in a fully ordered spinel.

The total enthalpy of the configuration is then given by $E = E_J + E_μ$. Collecting together terms in x and x^2 to facilitate comparison between this and the O'Neill-Navrotsky model, and writing $\Sigma J_{TT} = 4J_{1,TT} + 12J_{2,TT} + 12J_{3,TT} + 6J_{4,TT}$, $\Sigma J_{OO} = 6J_{1,OO} + 12J_{2,OO} + 12J_{3,OO} + 12J_{4,OO}$, and $\Sigma J_{TO} = 12J_{1,TO} + 16J_{2,TO} + 12J_{3,TO} + 36J_{4,TO}$ for convenience,

$$E = x^2\left(N_T\sum J_{TO} - N_T\sum J_{TT} - \frac{N_O}{4}\sum J_{OO}\right)$$
$$+ x\left(N_T\sum J_{TT} + \frac{N_O}{2}\sum J_{OO} - \frac{3N_T}{2}\sum J_{TO} + N_T μ\right) \tag{8}$$
$$+ N_T\sum J_{TO}$$

We therefore note that the O'Neill-Navrotsky α and β parameters each depend on all types of J values, but the chemical potential contributes to the α parameter only. In addition, our model contains a constant term, which is absent from the O'Neill-Navrotsky model. We will therefore compare our model with the O'Neill-Navrotsky model by offsetting our model enthalpy such that it has a zero value at $x = 0$, $Q = 1$. It is also possible to compare directly the two models with MC simulations, but only for the $Q = 1$ case, as this is the only case in which short range order is necessarily absent.

Examining Equation 8, we can also draw conclusions about the sign of β. The x^2 term in Equation 8 contains contributions from T-T, O-O, and T-O interactions. The T-T and O-O contributions are both negative, whilst the T-O contribution is positive. It can therefore be deduced that the sign of β is dependent on the relative strengths of the (T-T + O-O) interactions vs. the strength of the T-O interactions (assuming all are of the same sign, as demonstrated below).

TABLE 2. Parameters used as input for VCA models for GULP optimizations, and comparison with optimized values

Composition	Source	Initial a (Å)	Final a (Å)	% diff	Initial u	Final u	% diff
$MgAl_2O_4$	Redfern et al. (1999), 299 K sample, Table 1	8.0836	7.971092	−1.39	0.26171	0.257913	1.45
$MgFe_2O_4$	O'Neill et al. (1992), 450 °C sample, Tables 1 and 4	8.3806	8.232223	−1.77	0.2557	0.257904	0.86
$FeAl_2O_4$	Harrison et al. (1998), 298 K sample, Table 1	8.14578	7.924887	−2.71	0.26245	0.257862	1.75
Fe_3O_4	O'Neill and Dollase (1994), Table 9	8.397	8.194681	−2.41	0.255	0.257854	1.12
$NiAl_2O_4$	O'Neill et al. (1991), 700 °C sample, Table 2	8.0452	7.962662	−1.03	0.2549	0.258195	1.29
$NiFe_2O_4$	Subramanyam (1971)	8.3379	8.227229	−1.33	0.256	0.25815	0.84
$ZnAl_2O_4$	O'Neill and Dollase (1994), 900 °C sample, Table 8	8.0865	8.104044	0.22	0.2646	0.257814	2.56
$ZnFe_2O_4$	O'Neill (1992), 500 °C sample, Table 3	8.4419	8.364462	−0.92	0.2604	0.257817	0.99

We can use the model expression to predict whether, with a particular set of parameters and a particular starting configuration, we will obtain a normal or inverse spinel. In some cases, the O'Neill-Navrotsky model coefficients predict a lower enthalpy for a normal spinel when an inverse configuration is expected. For example, the values obtained by O'Neill et al. (1992) for $MgFe_2O_4$, $\alpha = 26.6$ and $\beta = -21.7$ kJ/mol, give the curve shown in Figure 1 for the enthalpy as a function of Q, in which the enthalpy of the ordered spinel is lower than that of the inverse spinel, despite the fact that $MgFe_2O_4$ is observed to adopt the inverse structure. This may seem counterintuitive; however, if we examine the free energy as predicted by Equation 3, the situation becomes clearer. Figure 2 shows the free energies of a normal spinel ($MgAl_2O_4$) and an inverse spinel ($MgFe_2O_4$) as predicted by Equation 3 at 100, 500, 1000, and 5000 K. The higher entropy of the inverse structure is a factor in stabilizing it relative to the normal structure. Our simulations (discussed in more detail below) are started off in a random configuration ($Q = 0$, shown by the vertical dotted lines on Fig. 2) and allowed to equilibrate at each temperature. One can note from Figure 2 that at 100 K, the global free energy minimum is the normal configuration for both $MgAl_2O_4$ and $MgFe_2O_4$. Hence, a simulation of $MgAl_2O_4$ started with a random configuration will simply evolve down the free energy gradient to $Q = 1$. However, for $MgFe_2O_4$, despite the fact that the free energy of the normal case is lower than that of the inverse case, the maximum in the free energy of $MgFe_2O_4$ at $Q \sim 0.1$ means that an initially random configuration will evolve toward $Q = -0.5$.

Monte Carlo (MC) simulations

The MC simulations were performed using the program OSSIA (Warren et al. 2001). For this program, the system is represented as a set of spins interacting with a specified topology and specified interaction/chemical potential energies (the J and μ values); these spins are then mapped onto the crystal structure as atoms at the end of the simulation.

We use the unlike interaction representation, in which A-A and B-B interactions are not defined, but A-B (and B-A) interactions take the values in Table 3.

All MC simulations reported in this paper used a $3 \times 3 \times 3$ supercell of the $2 \times 2 \times 2$ supercell used in the GULP calculations, i.e., with 648 cation sites. Initial simulations showed that the spin systems equilibrate quickly at a particular temperature, which meant that some intermediate simulations could be run with relatively few steps (typically 10^5–10^6). Final simulations were run with 2×10^7 steps—that is, 10^7 equilibration steps and 10^7 production steps.

Most of our simulations were initialized in a random state; at each temperature, each cation site is populated randomly with a cation in the specified proportions, and this is called a "hot start," since it is analogous to the expected high-temperature behavior, $Q = 0$. Alternatively, they may be initialized in a "cold start," whereby the user specifies the cation occupancy site by site. This is appropriate for a normal spinel, since there is only one possible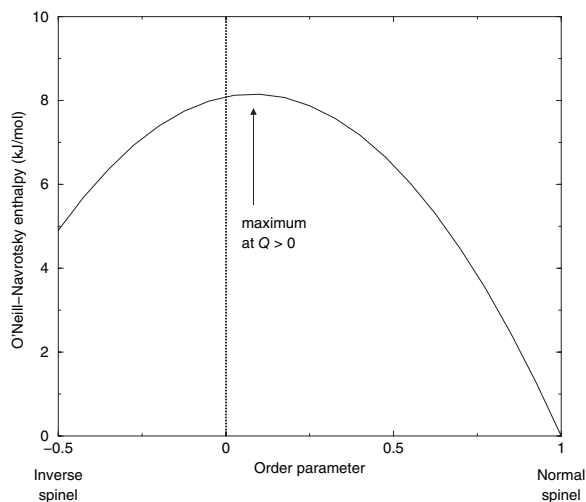 configuration (all tetrahedral sites occupied by A, all octahedral sites occupied by B), but more difficult for an inverse spinel, since although all tetrahedral sites are occupied by B, there are many possible configurations of 50% A and 50% B in the octahedral sites. However, it is possible to perform a hot start simulation to deduce a possible ordered structure, and then use that ordered structure as the starting structure for a cold start simulation. In any case, whether started in an ordered or disordered state, the system is given the opportunity to evolve toward an equilibrium state at a particular temperature.

RESULTS

J parameters for spinels

The values of J parameters and chemical potentials obtained for the spinels studied are given in Table 3. Figure 3 shows the J values graphically, and illustrates that there is a striking similarity between the values for all but $ZnAl_2O_4$. It is especially interesting to note that similar J values are obtained for both normal and inverse spinels, with only the chemical potential dictating the normal or inverse behavior. With the exception of $J_{1,TT}$, $J_{1,OO}$, and $J_{2,OO}$ in $ZnAl_2O_4$ and $J_{4,TT}$ in Fe_3O_4, all J values are negative, indicating that it is energetically favorable for A-B pairs to form, irrespective of their separation. This has the potential to create "frustration" in the system, since it is not possible for all pairs to be A-B, but in this case the nearest-neighbor interactions have the largest energy and therefore are dominant. It is also interesting to note that, for each of the T-T, O-O, and T-O interactions, there is a rapid decay in the strength of the interactions with distance; this is not necessarily always the case, e.g., in MC simulations of muscovite (Palin et al. 2001), third-nearest
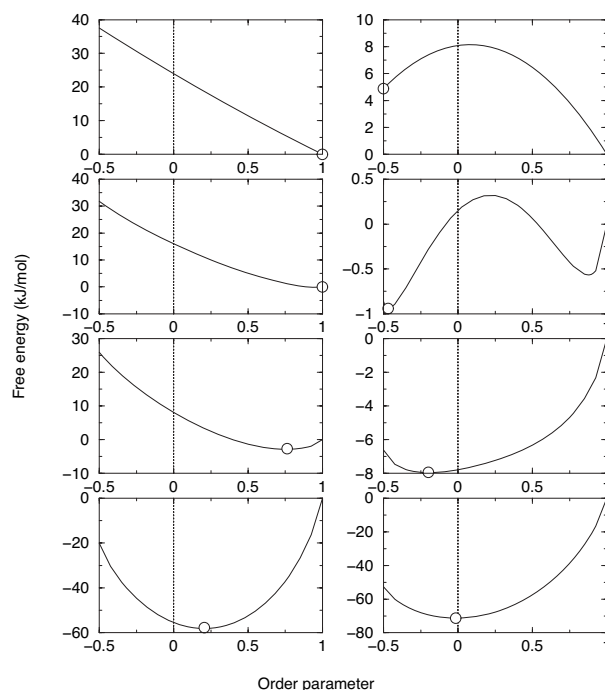

FIGURE 1. Ordering enthalpy of $MgFe_2O_4$ as given by O'Neill-Navrotsky model as a function of Q.

FIGURE 2. Free energy curves for $MgAl_2O_4$ (left) and $MgFe_2O_4$ (right), constructed from the O'Neill-Navrotsky model (Eq. 3) using $\alpha = 32.8$, $\beta = 4.7$ kJ/mol for $MgAl_2O_4$ (Redfern et al. 1999) and $\alpha = 26.6$, $\beta = -21.7$ kJ/mol for $MgFe_2O_4$ (O'Neill et al. 1992). Top to bottom: 100, 500, 1000, 5000 K. Circles represent equilibrium degree of inversion that would be obtained from an initially random cation configuration (vertical dotted lines).

neighbor interactions were found to be smaller than fourth-nearest neighbor interactions.

It is not clear at this point why the results for $ZnAl_2O_4$ are so different from those of the other seven spinels studied. The discrepancy may be due to the large value of μ, which makes a much larger contribution to the energy of ordering than that from the J values.

Random-mixing model results

Figure 4 shows the total enthalpy calculated from the random-mixing model, and the separate contributions from T-T, O-O, T-O, and μ, using the J and μ values for $MgAl_2O_4$. It can be seen that the contributions from T-T and O-O are concave curves, and that from T-O is a convex curve. The chemical potential is linear in x. The total enthalpy curve shows that the normal spinel is favored. An analogous plot for $MgFe_2O_4$ is shown in Figure 5; the main difference is that the chemical potential has opposite sign, which means that the inverse spinel is favored.

Also inset on Figures 4 and 5 are the enthalpies calculated using the O'Neill-Navrotsky model (as a function of Q rather than of x) compared with the total random-mixing enthalpies (shifted such that they have zero value at $Q = 1$). For $MgAl_2O_4$, the enthalpy curves from the two models have similar forms,
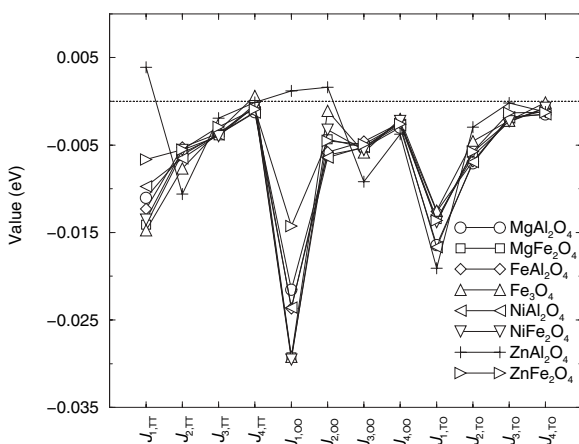
but the curves for $MgFe_2O_4$ are very different. In particular, the O'Neill-Navrotsky enthalpy is higher for the inverse case than for the normal case, suggesting that, although a model with these α and β parameters fits the experimental data, it predicts that the most stable configuration for $MgFe_2O_4$ is the normal configuration, as discussed above.

MC results: Comparison with previous study

One aim of this study is to determine to what extent the results of our simulation approach differ from those of Lavrentiev et al. (2003) who used a slightly different technique. Figure 6 uses $MgAl_2O_4$ and $MgFe_2O_4$ as examples of normal and inverse spinels, comparing our MC simulation results with those obtained by Lavrentiev et al. and also with experimental data for each spinel. It can be seen that there is no significant difference between the results of those authors and the results obtained in this work, and thus, a similar degree of agreement of simulations with experimental data. Lavrentiev et al. also presented MC results for $FeAl_2O_4$, $NiAl_2O_4$, and $ZnAl_2O_4$. These also compared favorably with our results; the results from the two simulations for $FeAl_2O_4$ were virtually identical, and our results for $NiAl_2O_4$
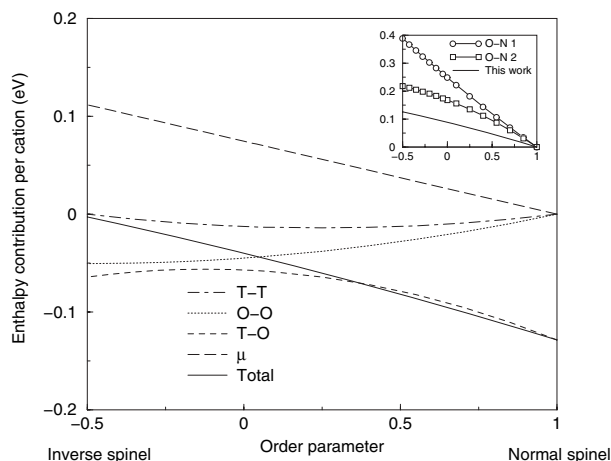

FIGURE 4. Random-mixing model enthalpy, and its components from T-T, O-O, and T-O interactions and chemical potential, for $MgAl_2O_4$. Inset: comparison of total enthalpies from random-mixing and O'Neill-Navrotsky models for $MgAl_2O_4$. Key to inset: "O–N 1" = α = 32.8, β = 4.7 kJ/mol (Redfern et al. 1999), "O–N 2" = α = 31, β = –10 kJ/mol (Peterson et al. 1991).

FIGURE 3. Calculated J values for all spinels studied in this work.

TABLE 3. Fitted parameters for various spinels

	$MgAl_2O_4$	$MgFe_2O_4$	$FeAl_2O_4$	Fe_3O_4	$NiAl_2O_4$	$NiFe_2O_4$	$ZnAl_2O_4$	$ZnFe_2O_4$
R^2	0.999974	0.999392	0.999976	0.997837	0.999578	0.999971	0.999984	0.999992
E_0	−8676.7(4)	−8368.6(6)	−8697.5(4)	−8387.0(8)	−8650.5(5)	−8346.0(6)	−8542(1)	−8240.0(4)
$J_{1,TT}$	−0.0110(5)	−0.0141(6)	−0.0123(5)	−0.0147(9)	−0.0097(5)	−0.0135(7)	0.0039(12)	−0.0066(4)
$J_{2,TT}$	−0.0061(3)	−0.0059(4)	−0.0053(3)	−0.0077(5)	−0.0065(3)	−0.0055(4)	−0.0106(7)	−0.0055(3)
$J_{3,TT}$	−0.0037(3)	−0.0039(4)	−0.0037(3)	−0.0034(5)	−0.0038(3)	−0.0040(4)	−0.0019(7)	−0.0029(3)
$J_{4,TT}$	−0.0012(3)	−0.0004(4)	−0.0007(3)	0.0006(5)	−0.0013(3)	−0.0006(4)	−0.0001(7)	−0.0009(3)
$J_{1,OO}$	−0.0215(3)	−0.0293(4)	−0.0237(3)	−0.0292(5)	−0.0236(3)	−0.0295(4)	0.0012(7)	−0.0143(3)
$J_{2,OO}$	−0.0061(2)	−0.0044(3)	−0.005(2)	−0.0011(4)	−0.0064(2)	−0.0033(3)	0.0016(5)	−0.0045(2)
$J_{3,OO}$	−0.0053(2)	−0.0053(3)	−0.0046(2)	−0.0059(4)	−0.0052(2)	−0.0056(3)	−0.0092(5)	−0.0049(2)
$J_{4,OO}$	−0.0030(2)	−0.0024(3)	−0.0025(2)	−0.0020(4)	−0.0027(2)	−0.0023(3)	−0.0038(5)	−0.0026(2)
$J_{1,TO}$	−0.0164(2)	−0.0135(3)	−0.0126(2)	−0.0125(4)	−0.0167(3)	−0.0138(3)	−0.0191(6)	−0.0136(2)
$J_{2,TO}$	−0.0071(2)	−0.0062(2)	−0.0068(2)	−0.0046(3)	−0.0069(2)	−0.0058(3)	−0.0030(4)	−0.0057(2)
$J_{3,TO}$	−0.0018(2)	−0.0023(3)	−0.0021(2)	−0.0022(4)	−0.0018(2)	−0.0023(3)	−0.0002(5)	−0.0013(2)
$J_{4,TO}$	−0.0015(1)	−0.0008(2)	−0.0011(1)	−0.0001(2)	−0.0015(1)	−0.0007(2)	−0.0012(3)	−0.0012(1)
μ	0.335(4)	−0.094(5)	0.378(4)	−0.057(7)	−0.126(4)	−0.496(6)	0.990(9)	0.538(3)

Notes: Interaction parameters J_i are for unlike interactions and the goodness of fit is illustrated by the R^2 correlation coefficient. All values in eV with standard error on the last digit given in parentheses.

were in slightly better agreement with experimental data. At high temperature, there was a discrepancy between the two simulations for $ZnAl_2O_4$, but this can probably be explained by the fact that the behavior at high temperature is more susceptible to fluctuation. As such, it appears that the specific inclusion of vibrational energy contributions by Lavrentiev et al. does not have a very large effect on the simulated cation distributions.

Parameter scaling

Since the O'Neill-Navrotsky model of ordering enthalpy as a function of x (or Q) produces good fits to experimental data, it is desirable to obtain similar $E(Q)$ curves from the random-mixing model we discussed above. One way of attempting to achieve this result is to scale the sets of parameters obtained from our GULP calculations. If this is to be done, however, it is prudent to scale only some parameters, since the various sets of parameters are all interdependent.

We investigated the effect of scaling parameters on both the $E(Q)$ curve from the model and the $Q(T)$ curve from the MC simulations. We selected $MgFe_2O_4$ as a suitable candidate for this test, since there are two independent experimental data sets available over relatively large temperature ranges.

We scaled the parameters in each set together, i.e., all T-T parameters by the same amount, all O-O parameters by the same amount, etc., but scaled each parameter set independently. We also scaled μ independently. MC simulations were performed with doubled and halved values of the parameters and compared with the initial MC simulation with all parameters unscaled.

Figure 7 shows the effect on $E(Q)$ and $Q(T)$ of these scalings for $MgFe_2O_4$. Doubling the T-T parameters produces a pronounced minimum in $E(Q)$, around $Q = -0.1$, which is reflected in the fact that in the MC simulation, the system does not become fully inverse, even at low temperature. Other scalings of T-T and O-O parameters do not appear to affect significantly the temperature at which disordering begins, although they do affect how disordered the system is at high temperatures. Scaling the T-T parameters does not affect the enthalpies of ordered and inverse states, and scaling the O-O parameters affects only the inverse enthalpy, not the ordered enthalpy.

Scaling the T-O parameters, however, affects the position with respect to temperature of the steepest part of the $Q(T)$ curve, between the ordered and disordered regimes. There is also an effect on the degree of disorder at high temperatures. The enthalpy of both the ordered and inverse states also changes with different T-O scale factors. This suggests that the T-O parameters would be the most useful ones to scale in terms of fitting the experimental data.

Scaling μ by a positive factor appears to have a similar effect on $Q(T)$ as scaling the O-O parameters, but will not affect the curvature of $E(Q)$, as μ affects only the part of the enthalpy that is linear in x.

We have not considered the possibility of scaling the parameters by negative scale factors. Scaling the J values by a negative factor would be nonsensical, because it would reverse the preference for unlike cation interactions over like cation interactions. Similarly, the sign of μ obtained from the GULP calculations is correct for all eight spinels, again making it illogical to reverse it.

We concluded from this that scaling both the T-O parameters and μ by positive scale factors should provide us with control over (1) the temperature location of the steepest part of the $Q(T)$ curve; (2) the slope of the steepest part of the $Q(T)$ curve; (3) the curvature of the $E(Q)$ curve, including the location of any maxima or minima that might affect whether an initially disordered system evolves toward normal or inverse configuration; and (4) the relative enthalpies of normal and inverse spinels. In this scheme, varying μ and $J_{i,TO}$ to best fit the data using the Monte Carlo simulations is analogous to varying α and β to best fit the data using the O'Neill-Navrotsky model.

Figure 8 shows the results of MC simulations for all eight spinels studied in this work, compared with available experimental data (see figure caption for references). In the cases of $MgAl_2O_4$ and $FeAl_2O_4$, the agreement with experiment was sufficiently good that no parameter scaling was necessary. For $MgFe_2O_4$, Fe_3O_4, $NiAl_2O_4$, $ZnAl_2O_4$, and $ZnFe_2O_4$, results are
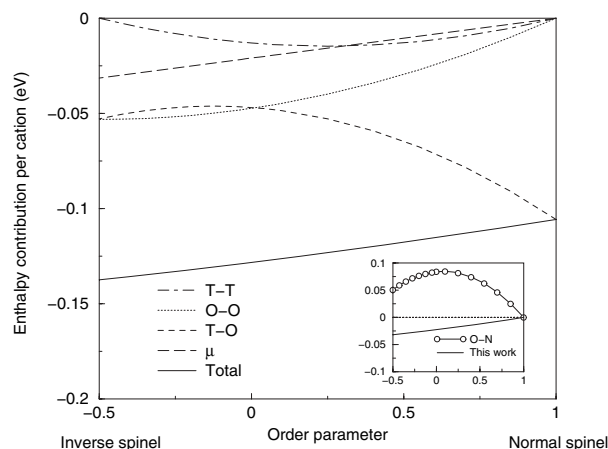

FIGURE 5. Random-mixing model enthalpy, and its components from T-T, O-O, and T-O interactions and chemical potential, for $MgFe_2O_4$. Inset: comparison of total enthalpies from random-mixing and O'Neill-Navrotsky model for $MgFe_2O_4$. Key to inset: "O–N" = α = 26.6, β = –21.7 kJ/mol (O'Neill et al. 1992).
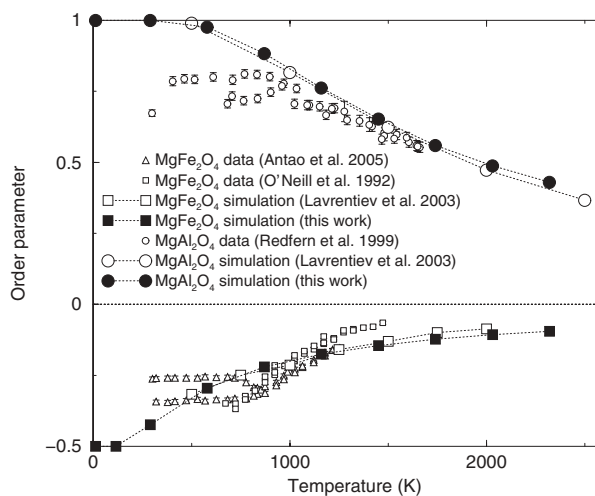

FIGURE 6. Comparison of MC results from this study, MC results of Lavrentiev et al. (2003), and experimental results for $MgAl_2O_4$ and $MgFe_2O_4$.

FIGURE 7. Effect of scaling parameter sets on $E(Q)$ (from model) and $Q(T)$ (from MC simulation) for $MgFe_2O_4$. Top to bottom: scaling T-T only, scaling O-O only, scaling T-O only, scaling μ only. Curves without symbols indicate the initial, unscaled result; curves with large and small symbols represent doubling and halving the parameters, respectively.
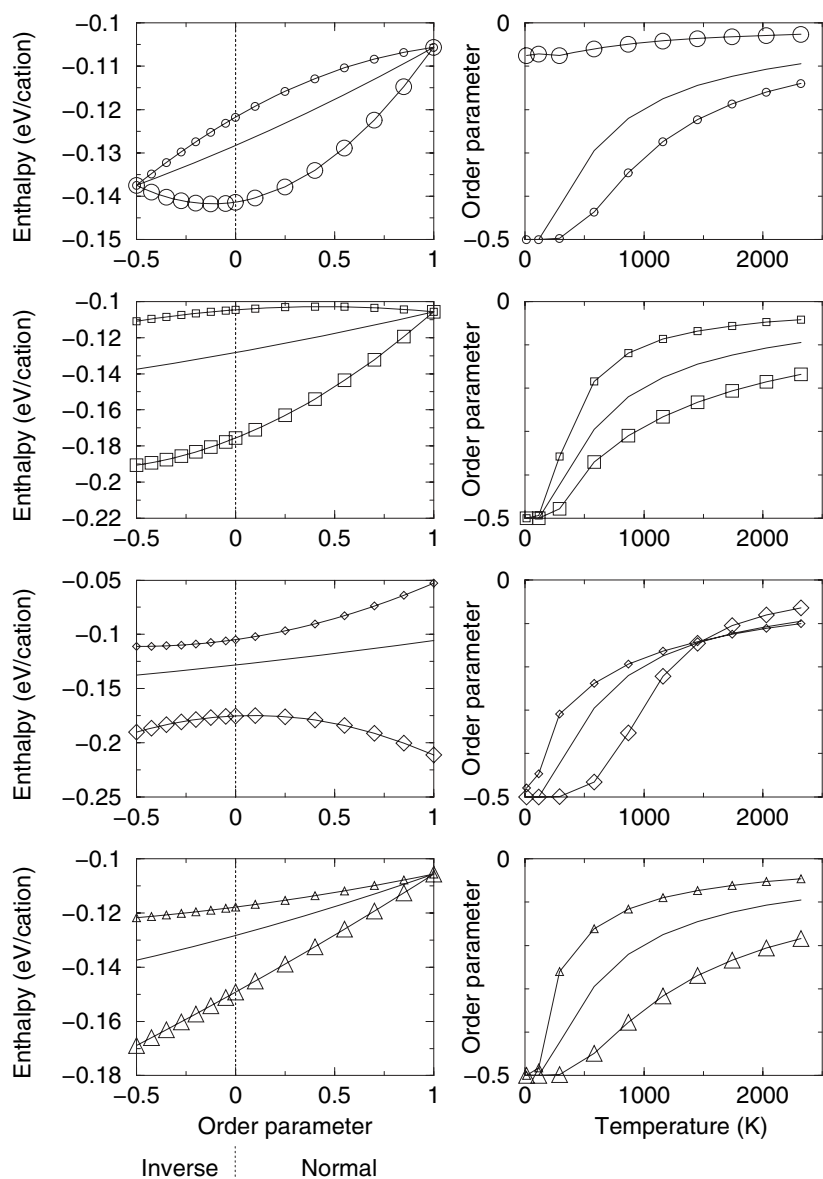

shown both for unscaled and scaled parameters. In all cases except magnetite, the fit was obtained by scaling up the T-O interactions and scaling down μ (in the case of magnetite, μ was increased). The scaling factors used for each case are given in the figure caption. The agreement between experimental data and MC results with scaled parameters is mostly very good (points where experimental samples have not equilibrated have been excluded when judging the goodness of fit), although for magnetite it was not possible to obtain such a good fit to the data, presumably because of the significant contribution of the magnetic interactions to the ordering behavior of magnetite. In the case of $NiFe_2O_4$, no experimental data are available, since this is a very rare mineral, but the MC results are included for completeness.

Figure 9 shows the computed J values for all the spinels studied in this work, analogously to Figure 3, but with the T-O interactions scaled by the factors used in the MC simulations. A comparison of Figures 3 and 9 serves to illustrate that only modest adjustments to the T-O interactions were necessary to achieve a good fit to the experimental data, and that the overall pattern of absolute and relative values of T-T, O-O, and T-O interactions from the original GULP calculations is essentially retained. The comparison indicates that T-O interactions were slightly underestimated by the original GULP calculations, which was responsible for the generally poor fit to the experimental data. After scaling, the T-O interactions become of similar magnitude to the O-O interactions.

Comparison between models, and the issue of short-range order

Figure 10 compares O'Neill-Navrotsky $E(Q)$ curves with model curves computed with unscaled and scaled (where applicable) parameters. Also included for comparison are the enthalpies from the MC simulations.

The main point to note from these plots is that the MC results for the normal spinels follow exactly the theoretical behavior from the random-mixing model. The MC results for the inverse spinels, however, do not; the MC enthalpy is always lower than that predicted by the random-mixing model. This is indicative of the presence of short-range order. It is possible to quantify the degree of short-range order by using the technique of thermodynamic integration (see e.g., Warren et al. 2001), by which it is possible to calculate the free energy and hence the entropy from the simulation results for the enthalpy. This can then be compared with the expected configurational entropy of the system as a function of temperature, computed via Equation 2 from x, which is in turn obtained from the simulated Q value at each temperature.

Figure 11 shows thermodynamic integration results for $MgAl_2O_4$ and $MgFe_2O_4$. For $MgAl_2O_4$, there is almost no difference between the entropies from the two approaches, and hence there is almost no short-range order in $MgAl_2O_4$. The results for the other normal spinels showed a similar lack of short-range order. A previous study of cation ordering in $MgAl_2O_4$ via an
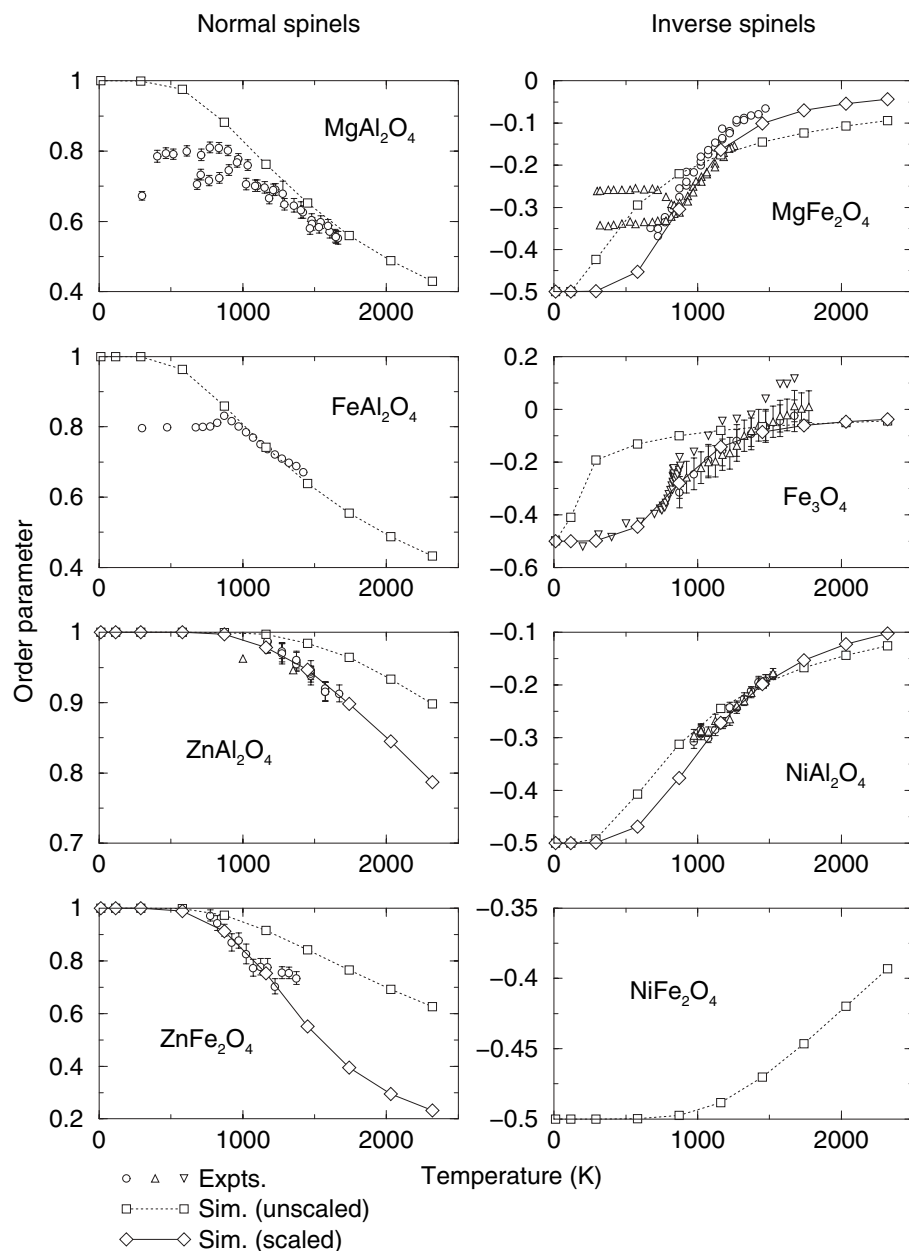
FIGURE 8. MC simulation results and comparison with experimental data for all spinels studied in this work. Experimental data are from the following sources: $MgAl_2O_4$ = Redfern et al. (1999); $FeAl_2O_4$ = Harrison et al. (1998); $ZnAl_2O_4$ = O'Neill and Dollase (1994) (circles), Waerenborgh et al. (1994) (triangles); $ZnFe_2O_4$ = O'Neill (1992); $MgFe_2O_4$ = O'Neill et al. (1991) (circles), Antao et al. 2005 (triangles); Fe_3O_4 = Nell et al. (1989) (circles), Wu and Mason (1981) (up triangles), Wissmann et al. (1998) (down triangles); $NiAl_2O_4$ = O'Neill et al. (1991) Mo$K\alpha$ radiation (circles), Cu$K\alpha$ radiation (triangles). There are no $NiFe_2O_4$ data available for comparison. Where error bars are not shown on experimental data points, they are comparable with, or smaller than, the symbol size. Simulation parameter scalings are as follows: $ZnAl_2O_4 = 0.7 \times \mu$; $ZnFe_2O_4 = 1.75 \times J_{i,TO}$ and $0.1 \times \mu$; $MgFe_2O_4 = 2 \times J_{i,TO}$ and $0.87 \times \mu$; $Fe_3O_4 = 2.6 \times J_{i,TO}$ and $1.8 \times \mu$; $NiAl_2O_4 = 1.5 \times J_{i,TO}$ and $0.9 \times \mu$.

ab initio approach (Warren et al. 2000a, 2000b) showed a very similar $S(T)$ curve, but did not assess explicitly the degree of short-range order.

For $MgFe_2O_4$, the entropy calculated via thermodynamic integration is lower than that expected from the configurational entropy calculation, meaning that there is significant short-range order in $MgFe_2O_4$. The other inverse spinels behaved analogously.

Figure 12 illustrates the amount of short-range order in $MgFe_2O_4$, $NiAl_2O_4$, and Fe_3O_4, simply as the difference between the expected configurational entropy and the actual entropy from the thermodynamic integration. At very low temperatures, there is complete order, so the actual entropy is zero, and since $x = 1$, the expected configurational entropy is $2R\ln2$ (11.5 kJ/mol). Hence the entropy difference is constant at $2R\ln2$ initially, but

on increasing temperature, there are sudden decreases at ~120 K ($NiAl_2O_4$), ~170 K ($MgFe_2O_4$), and ~230 K (Fe_3O_4). The form of these curves is very similar to the short-range order parameter plots computed by Seko et al. (2006) for $MgGa_2O_4$ and $MgIn_2O_4$; these authors noted an abrupt decrease in the short-range order parameter which they attributed to the onset of long-range ordering of cations on octahedral sites.

Long-range order in inverse spinels

Snapshots of the fully ordered structure obtained from the MC simulations of $MgFe_2O_4$ at temperatures lower than ~170 K is shown in Figure 13 (note that no O atoms are present as these are not included in the MC simulation). The Mg atoms form chains along one direction in the unit cell; these chains have 4_1 symmetry.
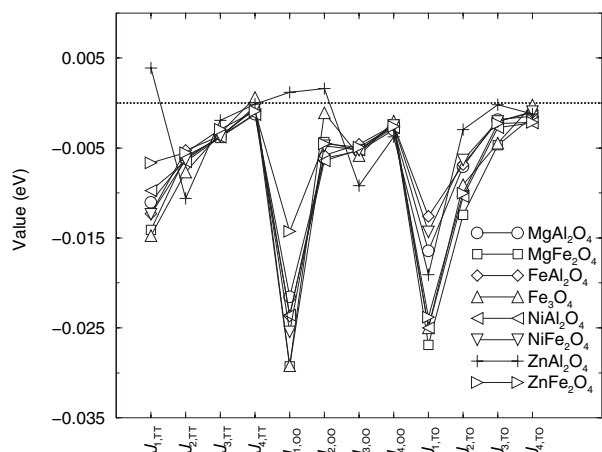
FIGURE 9. *J* values for all spinels studied in this work, with T-O parameters scaled.

We can examine the long-range ordering in our simulations by considering the cation site occupancies as a function of temperature. Figure 14 shows the average Fe contents of sites in $MgFe_2O_4$, computed from the MC simulations. The average tetrahedral and octahedral Fe site fractions change rather smoothly. However, the average octahedral Fe content can in turn be split into two parts. One part is the average site occupancy for sites where Fe is expected to occur in the long-range-ordered state, and the other is the average site occupancy for sites where Mg is expected to occur in the long-range-ordered state. From this, one can note that, at ~170 K, there is a discontinuity, with distinct occupancies of either Fe or Mg (i.e., 0 or 1 on the Figure) suddenly changing to roughly 0.5, i.e., statistically disordered octahedral sites.

To investigate further this long-range ordering, we optimized the geometry of the ordered structure (O atoms now included once more) using GULP, with the relevant potentials from Lavrentiev et al. (2003). The structural parameters of the
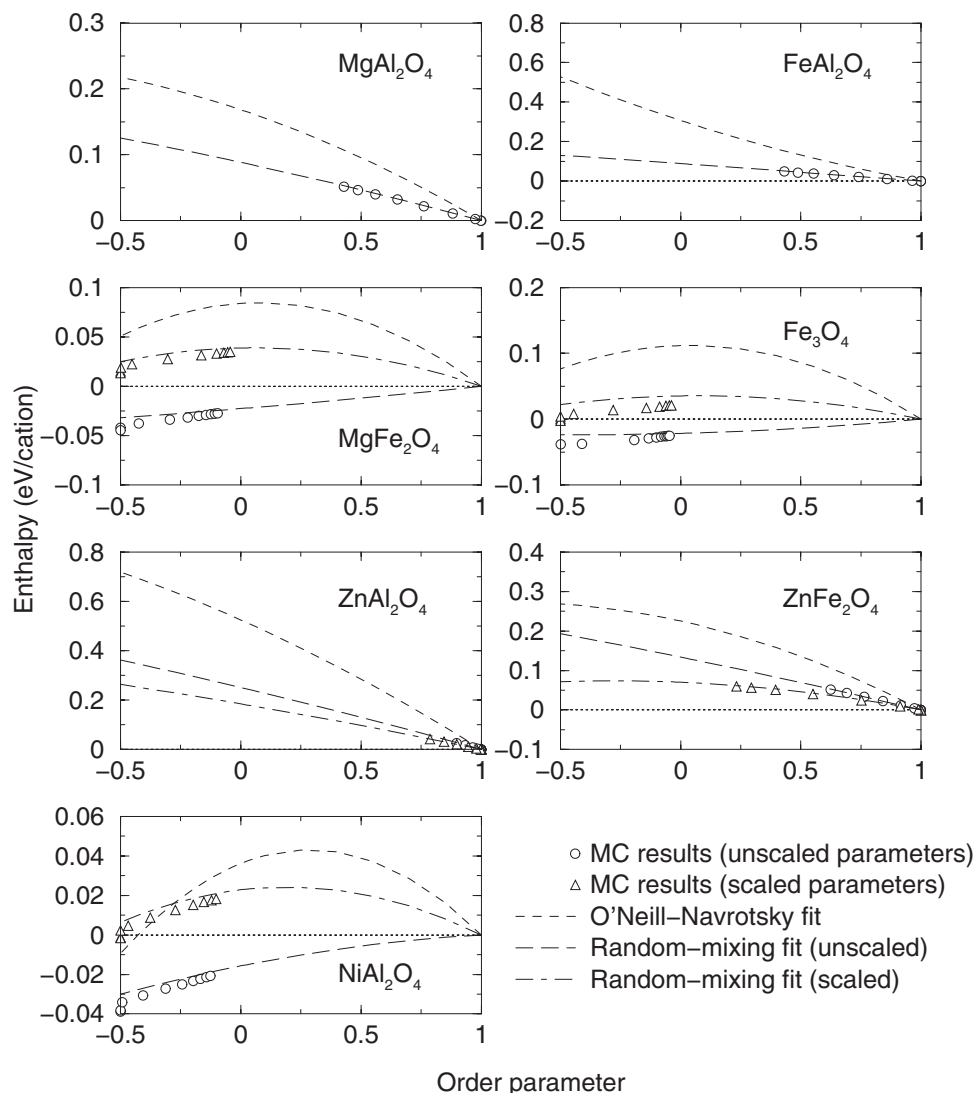

FIGURE 10. Comparison of O'Neill-Navrotsky model, random-mixing model, and actual MC simulation results for spinels. For the random-mixing model and MC results, curves are shown using both the unscaled and the scaled values of *J* values and μ. All results have been adjusted so that $E(Q=0)=0$. O'Neill-Navrotsky fits: $MgAl_2O_4$ = Redfern et al (1999), $FeAl_2O_4$ = Harrison et al (1998), $MgFe_2O_4$ = O'Neill et al (1992), Fe_3O_4 = Nell et al (1989), $ZnAl_2O_4$ = O'Neill and Dollase (1994), $ZnFe_2O_4$ = O'Neill (1992), and $NiAl_2O_4$ = O'Neill et al. (1991).
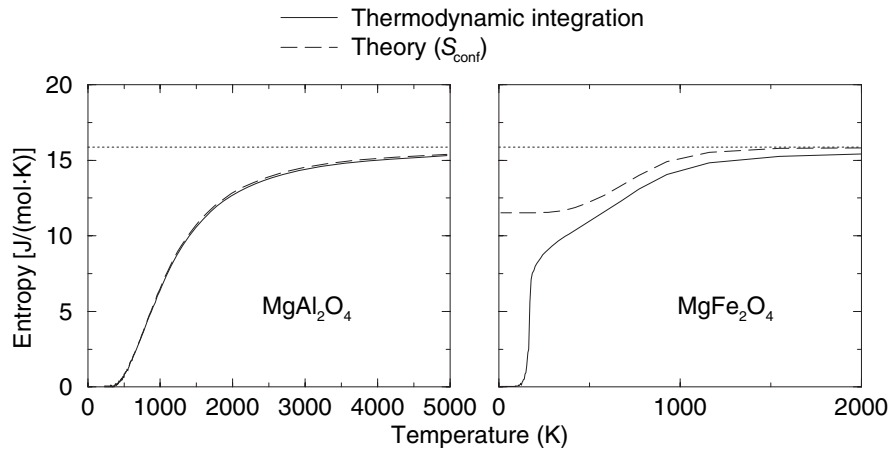
FIGURE 11. Thermodynamic integration results for MgAl$_2$O$_4$ and MgFe$_2$O$_4$, compared with expected configurational entropy (S_{conf}) computed from simulated order parameter. Dotted lines show maximum possible entropy of the system.

relaxed structure are given in Table 4. The ordered structure, with space group $P4_122$, and cell parameters $\sim\sqrt{2}a_c \times \sqrt{2}a_c \times a_c$ is identical to that obtained for the 4-2 spinels Mg$_2$TiO$_4$ and Zn$_2$TiO$_4$ (Millard et al. 1995) and analogous to that obtained for Mn$_2$TiO$_4$ (Bertaut and Vincent 1968), where the space group is $P4_322$ and the handedness of the chains of A (Ti) atoms is opposite to that of the chains of A atoms in MgFe$_2$O$_4$, Mg$_2$TiO$_4$, and Zn$_2$TiO$_4$. Similarly, Seko et al. (2006) determined by ab initio methods that the ordered inverse spinels MgGa$_2$O$_4$ and MgIn$_2$O$_4$ have the $P4_322$ space group. Burns et al. (1997) observed the space group $P4_122$ for an aluminous magnesioferrite, but they attributed the tetragonal nature to strain due to lattice mismatch resulting from the microstructural evolution of the sample, rather than to cation ordering.

DISCUSSION AND CONCLUSIONS

In this work we have shown that an atomistic approach can be used successfully to model cation order-disorder in 2-3 spinels. Some scaling of simulation parameters is necessary to reproduce experimental data, but in the cases where parameters were scaled, they were scaled similarly for all spinels (i.e., increased T-O interactions, decreased μ). The only exception was the case of magnetite, where magnetic interactions are likely to have a large effect, but such interactions are not included in our model. It is our intention to consider magnetic interactions in spinels at a later date.

By way of further discussion, we refer back to the questions we posed above.

Why does the O'Neill-Navrotsky model work so well for end-member 2-3 spinels?

The O'Neill-Navrotsky model consists of two terms, representing enthalpy and entropy. Therefore, the only possible way in which the model could fail is if it did not model sensibly one or both of these components. The enthalpy term is modeled as the sum of a linear and a quadratic part, which we have shown can be interpreted as a combination of T-T, O-O, and T-O interactions.

The entropy term is modeled as the configurational entropy, and we have shown above that there may be a significant discrep-
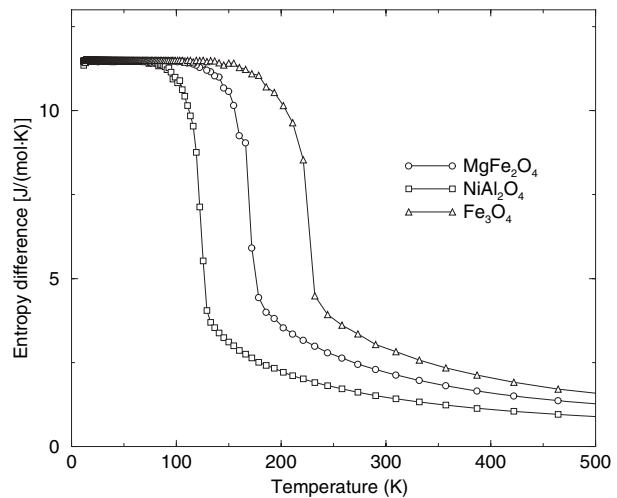

FIGURE 12. Difference between actual entropy (from thermodynamic integration) and predicted entropy S_{conf} for three inverse spinels.

TABLE 4. Details of optimized cation-ordered structure of MgFe$_2$O$_4$ as obtained from GULP

Space group	$P4_122$		
Lattice parameters	$a = 5.8309$ Å	$c = 8.2218$ Å	$\alpha = 90°$
Fractional coordinates:			
Atom	x	y	z
Fe	0.7425	0	0.25
Fe	0.25317	0.25317	0.375
Mg	0.25756	0.5	0.75
O	0.25971	0.96702	0.50693
O	0.73983	0.47624	0.02034

ancy between the expected configurational entropy and the actual entropy of the system. In other words, there may be considerable short-range order present in the system, but this phenomenon is not accounted for by the O'Neill-Navrotsky model.

However, the coefficients for the model are obtained by fitting to experimental data, and it turns out that entropy effect is not large when one is considering only the temperature range in which experimental data exist for spinels. In the case of normal
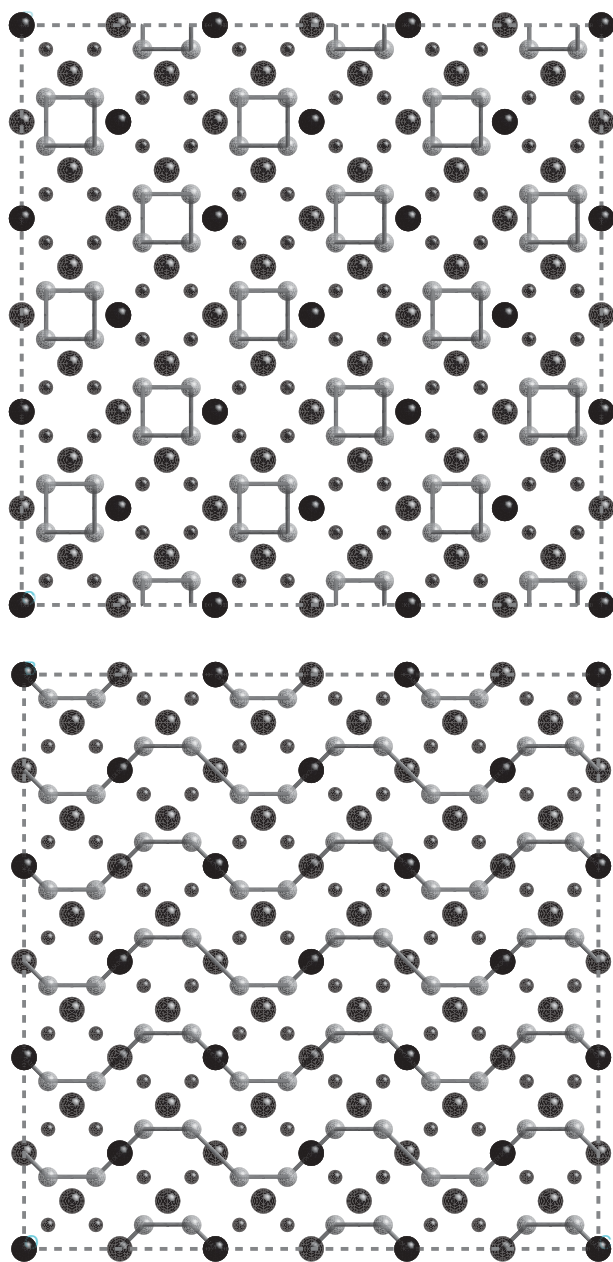
FIGURE 13. MC simulation snapshots (top: viewed along *z*, bottom: viewed along *x*) for MgFe$_2$O$_4$ at very low temperature. Gray = Mg (all octahedral), large black = tetrahedral Fe, small black = octahedral Fe. Artificial bonds have been drawn between Mg atoms as a visual aid.

FIGURE 14. Averaged Fe content of tetrahedral and octahedral sites in MgFe$_2$O$_4$. The average octahedral Fe content is in turn broken down into average Fe contents of octahedral sites, which at low temperature are occupied by Fe and Mg, respectively, denoted "Fe" [6] and "Mg" [6]. Note logarithmic scale on the *x*-axis.

spinels, we found that there was no discernible difference between the predicted and actual entropies in normal spinels across a very wide temperature range, and hence there is no discernible short-range order in normal spinels. Therefore, no discrepancy is expected between the O'Neill-Navrotsky model and the experimentally observed data for normal spinels—i.e., the model should work well. In the case of inverse spinels, the considerable short-range order that may exist is found at temperatures, which
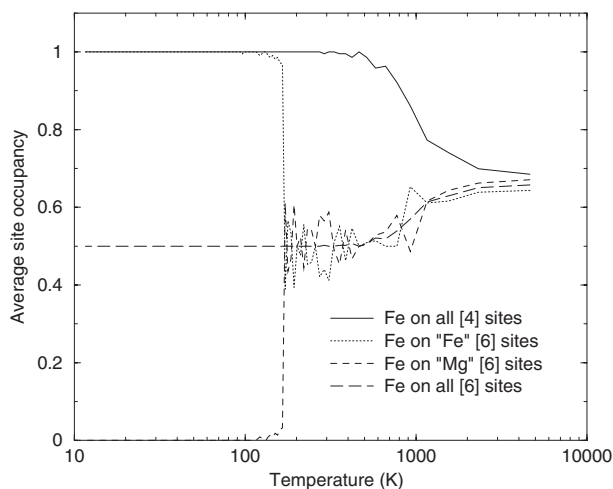
are experimentally inaccessible (i.e., <230 K). In the temperature range 700–1700 K, which we might consider as experimentally accessible, the difference between predicted and actual entropy of inverse spinels is only ~5–10% of the theoretical maximum difference of 2Rln2 (for a long-range-ordered spinel), and this is effectively insignificant. Therefore, the model should work well for inverse spinels as well.

What controls the values of α and β in the model?

We have gained some insights into the controls on the α and β parameters in the O'Neill-Navrotsky model by comparing it with our random-mixing model. Specifically, all types of interactions contribute to both α and β, but the chemical potential contributes to α only. Furthermore, the sign of β in the O'Neill-Navrotsky model is determined by the relative strengths of the (T-T + O-O) interactions vs. the T-O interactions.

What differences are there between our results and those of Lavrentiev et al. (2003)?

We found that we had to scale some of our Monte Carlo parameters to improve our MC fits to the data; using unscaled parameters, our results were generally similar to the previous work by Lavrentiev et al. When scaling, the important relationship appears to be the relative strengths of O-O vs. T-O interactions; we chose to vary this by scaling the T-O interactions rather than the O-O interactions, as this facilitated fitting to the experimental data. It is clear that GULP does not predict the relative strengths of O-O and T-O interactions very well, and we believe that the same issue underlies the results of Lavrentiev et al.

In summary, we have developed a consistent approach for modeling the thermodynamics of end-member 2-3 spinels. We plan to perform an analogous study on end-member 4-2 spinels, and this will be the subject of a future paper.

REFERENCES CITED

Antao, S.M., Hassan, I., and Parise, J.B. (2005) Cation ordering in magnesioferrite, $MgFe_2O_4$, to 982 °C using in situ synchrotron X-ray powder diffraction. American Mineralogist, 90, 219–228.

Arvidson, R.S. and Luttge, A. (2004) Kinetic Monte Carlo modeling of calcite dissolution kinetics. Geochimica et Cosmochimica Acta, 68, A125.

Bertaut, E.F. and Vincent, H. (1968) Etude par diffraction neutronique de la forme ordonnée de l'orthotitanate de manganese—structure cristalline et structure magnetique. Solid State Communications, 6, 269–275.

Bosenick, A., Dove, M.T., and Geiger, C.A. (2000) Simulation studies on the pyrope-grossular solid solution. Physics and Chemistry of Minerals, 27, 398–418.

Bosenick, A., Dove, M.T., Myers, E.R., Palin, E.J., Sainz-Díaz, C.I., Guiton, B., Warren, M.C., Craig, M.S., and Redfern, S.A.T. (2001) Computational methods for the study of energies of cation distributions: applications to cation-ordering phase transitions and solid solutions. Mineralogical Magazine, 65, 193–219.

Burns, P.C., Hawthorne, F.C., Libowitzky, E., Bordes, N., and Ewing, R.C. (1997) Donathite discredited: a mixture of two spinels. Neues Jahrbuch für Mineralogie—Monatshefte, 4, 163–174.

Cuadros, J., Sainz-Díaz, C.I., Ramirez, R., and Hernandez-Laguna, A. (1999) Analysis of Fe segregation in the octahedral sheet of bentonitic illite-smectite by means of FT-IR, ^{27}Al MAS-NMR and reverse Monte Carlo simulations. American Journal of Science, 299, 289–308.

Gale, J.D. (1997) GULP: a computer program for the symmetry-adapted simulation of solids. Journal of the Chemical Society: Faraday Transactions, 93, 629–637.

Harrison, R.J. (2006) Microstructure and magnetism in the ilmenite-hematite solid solution: a Monte Carlo simulation study. American Mineralogist, 91, 1006–1024.

Harrison, R.J., Redfern, S.A.T., and O'Neill, H.St.C. (1998) The temperature dependence of the cation distribution in synthetic hercynite ($FeAl_2O_4$) from in-situ neutron structure refinements. American Mineralogist, 83, 1092–1099.

Lavrentiev, M.Yu., Purton, J.A., and Allan, N.L. (2003) Ordering in spinels—a Monte Carlo study. American Mineralogist, 88, 1522–1531.

Millard, R.L., Peterson, R.C., and Hunter, B.K. (1995) Study of the cubic to tetragonal transition in Mg_2TiO_4 and Zn_2TiO_4 spinels by ^{17}O MAS NMR and Rietveld refinement of X-ray diffraction data. American Mineralogist, 80, 885–896.

Nell, J., Wood, B.J., and Mason, T.O. (1989) High-temperature cation distributions in Fe_3O_4-$MgAl_2O_4$-$MgFe_2O_4$-$FeAl_2O_4$ spinels from thermopower and conductivity measurements. American Mineralogist, 74, 339–351.

O'Neill, H.St.C. (1992) Temperature dependence of the cation distribution in zinc ferrite ($ZnFe_2O_4$) from powder XRD structural refinements. European Journal of Mineralogy, 4, 571–580.

O'Neill, H.St.C. and Dollase, W.A. (1994) Crystal structures and cation distributions in simple spinels from powder XRD structural refinements—$MgCr_2O_4$, $ZnCr_2O_4$, Fe_3O_4 and the temperature dependence of the cation distribution in $ZnAl_2O_4$. Physics and Chemistry of Minerals, 20, 541–555.

O'Neill, H.St.C. and Navrotsky, A. (1983) Simple spinels: crystallographic parameters, cation radii, lattice energies, and cation distribution. American Mineralogist, 68, 181–194.

——— (1984) Cation distributions and thermodynamic properties of binary spinel solid solutions. American Mineralogist, 69, 733–753.

O'Neill, H.St.C., Dollase, W.A., and Ross, C.R. (1991) Temperature dependence of the cation distribution in nickel aluminate ($NiAl_2O_4$) spinel—a powder XRD study. Physics and Chemistry of Minerals, 18, 302–319.

O'Neill, H.St.C., Annersten, H., and Virgo, D. (1992) The temperature dependence of the cation distribution in magnesioferrite ($MgFe_2O_4$) from powder XRD structural refinements and Mössbauer spectroscopy. American Mineralogist, 77, 725–740.

Palin, E.J., Dove, M.T., Redfern, S.A.T., Bosenick, A., Sainz-Díaz, C.I., and Warren, M.C. (2001) Computational study of tetrahedral Al–Si ordering in muscovite. Physics and Chemistry of Minerals, 28, 534–544.

Palin, E.J., Dove, M.T., Redfern, S.A.T., Guiton, B.S., Welch, M.D., and Craig, M.S. (2003a) Computer simulation of Al–Mg ordering in glaucophane and a comparison with infrared spectroscopy. European Journal of Mineralogy, 15, 893–901.

Palin, E.J., Dove, M.T., Redfern, S.A.T., Sainz-Díaz, C.I., and Lee, W.T. (2003b) Computational study of tetrahedral Al–Si and octahedral Al–Mg ordering in phengite. Physics and Chemistry of Minerals, 30, 293–304.

Palin, E.J., Dove, M.T., Hernández-Laguna, A., and Sainz-Díaz, C.I. (2004) A computational investigation of the Al/Fe/Mg order-disorder behaviour in the dioctahedral sheet of phyllosilicates. American Mineralogist, 89, 164–175.

Palin, E.J., Dove, M.T., Welch, M.D., and Redfern, S.A.T. (2005) Computational investigation of Al/Si and Al/Mg ordering in aluminous tremolite amphiboles. Mineralogical Magazine, 69, 1–20.

Peterson, R.C., Lager, G.A., and Hitterman, R.L. (1991) A time-of-flight neutron powder diffraction study of $MgAl_2O_4$ at temperatures up to 1273 K. American Mineralogist, 76, 1455–1458.

Piana, S. and Gale, J.D. (2006) Three-dimensional kinetic Monte Carlo simulation of crystal growth from solution. Journal of Crystal Growth, 294, 46–52.

Redfern, S.A.T., Harrison, R.J., O'Neill, H.St.C., and Wood, D.R.R. (1999) Thermodynamics and kinetics of cation order in $MgAl_2O_4$ spinel up to 1600 °C from in situ neutron diffraction. American Mineralogist, 84, 299–310.

Sainz-Díaz, C.I., Palin, E.J., Dove, M.T., and Hernández-Laguna, A. (2003a) Monte Carlo simulations of ordering of Al, Fe, and Mg cations in the octahedral sheet of smectites and illites. American Mineralogist, 88, 1033–1045.

Sainz-Díaz, C.I., Palin, E.J., Hernández-Laguna, A., and Dove, M.T. (2003b) Octahedral cation ordering of illite and smectite. Theoretical exchange potential determination and Monte Carlo simulations. Physics and Chemistry of Minerals, 30, 382–392.

——— (2004) Effect of the tetrahedral charge on the order-disorder of the cation distribution in the octahedral sheet of smectites and illites by computational methods. Clays and Clay Minerals, 52, 357–374.

Seko, A., Yuge, K., Oba, F., Kuwabara, A., and Tanaka, I. (2006) Prediction of ground-state state structures and order-disorder phase transitions in II-III spinel oxides: a combined cluster-expansion method and first-principles study. Physical Review B, 73, 184117.

Subramanyam, K.N. (1971) Neutron and X-ray diffraction studies of certain doped nickel ferrites. Journal of Physics C: Solid State Physics, 4, 2266–2268.

Tucker, M.G., Keen, D.A., and Dove, M.T. (2001a) A detailed structural characterization of quartz on heating through the alpha-beta phase transition. Mineralogical Magazine, 65, 489–507.

Tucker, M.G., Squires, M.P., Dove, M.T., and Keen, D.A. (2001b) Dynamic structural disorder in cristobalite: neutron total scattering measurement and reverse Monte Carlo modeling. Journal of Physics: Condensed Matter, 13, 403–423.

Vinograd, V.L. and Sluiter, M.H.F. (2006) Thermodynamics of mixing in pyrope-grossular, $Mg_3Al_2Si_3O_{12}$-$Ca_3Al_2Si_3O_{12}$, solid solution from lattice dynamics calculations and Monte Carlo simulations. American Mineralogist, 91, 1815–1830.

Vinograd, V.L., Winkler, B., Putnis A., Kroll, A., Milman, V., Gale, J.D., and Fabrichnaya, O.B. (2006a) Thermodynamics of pyrope-majorite, $Mg_3Al_2Si_3O_{12}$-$Mg_4Si_4O_{12}$, solid solution from atomistic model calculations. Molecular Simulation, 32, 85–99.

Vinograd, V.L., Winkler, B., Wilson, D.J., Putnis, A., and Gale, J.D. (2006b) Monte Carlo simulation of mixing in $Ca_3Fe_2Ge_3O_{12}$-$Ca_4Ge_4O_{12}$ garnets and implications for the thermodynamic stability of pyrope-majorite solid solution. Physics and Chemistry of Minerals, 33, 533–544.

Waerenborgh, J.C., Figueiredo, M.O., Cabral, J.M.P., and Pereira, L.C.J. (1994) Temperature and composition dependence of the cation distribution in synthetic $ZnFe_yAl_{2-y}O_4$ ($0 \leq y \leq 1$) spinels. Journal of Solid State Chemistry, 111, 300–309.

Warren, M.C., Dove, M.T., and Redfern, S.A.T. (2000a) Disordering of $MgAl_2O_4$ spinel from first principles. Mineralogical Magazine, 64, 311–317.

——— (2000b) Ab initio simulations of cation ordering in oxides: application to spinel. Journal of Physics: Condensed Matter, 12, L43–L48.

Warren, M.C., Dove, M.T., Myers, E.R., Sainz- Díaz, C.I., Guiton, B.S., and Redfern, S.A.T. (2001) Monte Carlo methods for the study of cation ordering in minerals. Mineralogical Magazine, 65, 221–248.

Wissmann, S., Wurmb, V.V., Litterst, F.J., Dieckmann, R., and Becker, K.D. (1998) The temperature-dependent cation distribution in magnetite. Journal of Physics and Chemistry of Solids, 59, 321–330.

Wu, C.C. and Mason, T.O. (1981) Thermopower measurement of cation distribution in magnetite. Journal of the American Ceramic Society, 64, 520–522.